Anal. Chem. **2010,** *82,* 6919–6925

Electrochemical Modulation for Signal Discrimination in Surface Enhanced Raman Scattering (SERS)

Emiliano Cortés,*,† Pablo G. Etchegoin,*,‡ Eric C. Le Ru,‡ Alejandro Fainstein,§ María E. Vela,† and Roberto C. Salvarezza†

Instituto de Investigaciones Fisicoquímicas Teóricas y Aplicadas (INIFTA), Universidad Nacional de La Plata-CONICET, Sucursal 4 Casilla de Correo 16 (1900), La Plata, Argentina, The MacDiarmid Institute for Advanced Materials and Nanotechnology, School of Chemical and Physical Sciences, Victoria University of Wellington, PO Box 600, Wellington, New Zealand, Centro Atómico Bariloche and Instituto Balseiro, Comisión Nacional de Energía Atómica and Universidad Nacional de Cuyo, (8400) San Carlos de Bariloche, Río Negro, Argentina

Electrochemical modulation to induce controlled fluctuations in SERS signals is introduced as a method to discriminate and isolate different contributions to the spectra. The modulation—which can be changed in potential range, amplitude, and frequency—acts as a controllable "switch" to turn on, off, or change specific Raman signals which can then be correlated within the spectra by different fluctuation analysis techniques. Principal component analysis (PCA), either by itself or assisted by fast fourier transform (FFT) prefiltering, are shown to provide viable tools to isolate the different components of the spectra. Electrochemical modulation provides, therefore, a technique to study complex cases of coadsorption, and resolve problems of spectral congestion in SERS signals.

The links between surface-enhanced raman scattering (SERS)[1,2] and electrochemistry go all the way back to the discovery of the effect in the 1970s.[3−5] Since then, electrochemical studies have provided invaluable information on the details of the electronic interaction of molecules with the underlying metal substrate responsible for the SERS enhancement. Particularly important have been studies where the origin of the so-called "chemical enhancement"[6,7] in SERS can be discerned. From a more modern point of view, SERS and electrochemistry have diversified into a myriad of different areas that include the studies of coadsorption (multiple species), biological redox system,[8,9] corrosion, surface science,[10] fuel cells, electrocatalysis, electronic models for charge-transfer processes on surfaces,[11−16] and single-molecule or single hot-spot SERS,[17,18] to name only a few.[19,20] The simultaneous presence of the laser field with electric potentials and/or currents in the many different experimental configurations of substrates with simple, multiple, or tip-like electrodes, together with the variety of environmental variables (like pH or the exact nature of the electrolyte) produce the vast diversity of experimental situations found in the modern applications of SERS to electrochemistry. Tian and co-workers[20] provide a lucid summary of recent advances in SERS for electrochemical applications. It is argued in ref 20 in fact, that electrochemical systems are among the most complex one can study in SERS. The combination of electrochemical processes at interfaces with SERS make these systems particularly challenging, but undoubtedly very relevant to understand fundamental aspects in real analytical and bioanalytical applications. Last, but not least, there are several techniques under development in SERS that combine the basic elements of electrochemical experiments, even though they would not be strictly speaking considered as such. Examples of the latter are recent attempts to combine SERS and molecule transport proper-

* To whom correspondence should be addressed. E-mail: emilianocll@gmail.com (E.C.), pablo.etchegoin@vuw.ac.nz (P.G.E.).
† Universidad Nacional de La Plata-CONICET.
‡ Victoria University of Wellington.
§ Comisión Nacional de Energía Atómica and Universidad Nacional de Cuyo.

(1) Le Ru, E. C.; Etchegoin, P. G. *Principles of Surface Enhanced Raman Spectroscopy and Related Plasmonic Effects*; Elsevier: Amsterdam, 2009.
(2) Aroca, R. F. *Surface-Enhanced Vibrational Spectroscopy*; John Wiley & Sons: Chichester, 2006.
(3) Fleischmann, M.; Hendra, P. J.; McQuillan, A. *J. Chem. Phys. Lett.* **1974**, *26*, 163–166.
(4) Jeanmaire, D. L.; Van Duyne, R. P. *J. Electroanal. Chem.* **1977**, *84*, 1–20.
(5) Albrecht, M. G.; Creighton, J. A. *J. Am. Chem. Soc.* **1977**, *99*, 5215–5217.
(6) Otto, A. *Surface-Enhanced Raman Scattering: Classical and Chemical Origins*; Springer-Verlag: Berlin, 1984.
(7) Tian, Z. Q. *Faraday Discuss.* **2006**, *132*, 309.
(8) Murgida, D. H.; Hildebrandt, P. *Chem. Soc. Rev.* **2008**, *37*, 937–945.
(9) Hildebrandt, P.; Murgida, D. H. *Bioelectrochemistry* **2002**, *55*, 139.
(10) Cai, W. B.; Ren, B.; Li, X. Q.; She, C. X.; Liu, F. M.; Cai, X. W.; Tian, Z. Q. *Surf. Sci.* **1998**, *406*, 9–22.
(11) Gersten, J. I.; Birke, R. L.; Lombardi, J. R. *Phys. Rev. Lett.* **1979**, *43*, 147–150.
(12) Lombardi, J. R.; Birke, R. L.; Lu, T.; Xu, J. *J. Chem. Phys.* **1986**, *84*, 4174–4180.
(13) Xie, Y.; Wu, D. Y.; Liu, G. K.; Huang, Z. F.; Ren, B.; Yan, J. W.; Yang, Z. L.; Tian, Z. Q. *J. Electroanal. Chem.* **2003**, *554*, 417–425.
(14) Lombardi, J. R.; Birke, R. L. *Acc. Chem. Res.* **2009**, *42*, 734–742.
(15) Tognalli, N.; Fainstein, A.; Bonazzola, C.; Calvo, E. J. *J. Chem. Phys.* **2004**, *120*, 1905.
(16) Tognalli, N.; Scodeller, P.; Flexer, V.; Szamocki, R.; Ricci, A.; Tagliazucchi, M.; Calvo, E. J.; Fainstein, A. *Phys. Chem. Chem. Phys.* **2009**, *11*, 7412.
(17) dos Santos, D. P.; Andrade, G. F. S.; Temperini, M. L. A.; Brolo, A. G. *J. Phys. Chem. C* **2009**, *113*, 17737–17744.
(18) Shegai, T.; Vaskevich, A.; Rubinstein, I.; Haran, G. *J. Am. Chem. Soc.* **2009**, *131*, 14390.
(19) Tian, Z. Q.; Ren, B. *Annu. Rev. Phys. Chem.* **2004**, *55*, 197–229.
(20) Wu, D. Y.; Li, J. F.; Ren, B.; Tian, Z. Q. *Chem. Soc. Rev.* **2008**, *37*, 1025–1041.

10.1021/ac101152t
Published on Web 07/26/2010

ties,[21] or the use of electrostatic fields to control the adsorption/desorption of molecules on SERS substrates according to their cationic/anionic nature in solution.[17,22]

It is perhaps due to the complexity of the systems under study that despite all the accumulated work over the last decades the combination of SERS and electrochemistry is still undergoing methodological and analytical advances as a technique. There is a genuine need to develop both new and more advanced methods and analysis tools to attack the ever increasing complexity of the problems that are being investigated (in particular in bioelectrochemical areas). An early example of the latter is the technique of *potential averaged SERS* developed by Tian and co-workers[23] to address the problem of fast electrochemical processes and SERS monitoring of unstable species on the electrodes. Detection of intermediate species in electrochemical reactions by time-resolved SERS has also been tried by Lombardi et al.[24] A more recent example, on the other hand, is the introduction of local imaging of the electrochemical current by surface-plasmon resonances in ref 25. Many of these new techniques are not directly linked or applied to SERS,[26,27] even though they share the same basic elements; that is, the combination of electrochemistry with a detection technique based on surface plasmon resonances.[1]

This paper aims at a methodological development in the combination of SERS and electrochemistry. As such we shall show some basic examples of the technique we propose. To this end, we borrow ideas from well established techniques of *optical modulation*[28] by using the ability of electrochemistry to turn "on" and "off" Raman signals (by changing the resonance conditions of the reduced or oxidized states), as well as to introduce other (more subtle) spectral changes as a function of the applied potential. Variations in SERS signals with potential have been extensively studied in the literature. A common trait is the observation of changes in the overall intensity of the spectra (as the main consequence of the applied potential) when switching from oxidized to reduced species. As a result, changes in the intensity of the SERS spectra due to the oxidation state have been used as a detection parameter in nanobiosensing,[29] to check the permeability of phospholipid membranes[30] or thiol self-assembled monolayers,[31] and to evaluate integrity and redox behavior in proteins;[32] among others.

SERS provides a tool to monitor electrochemical phenomena at concentration levels (~nanomolars, and below) that cannot be followed either in the voltamperogram or with other techniques. Its sensitivity can, in fact, go routinely all the way down to single molecule levels.[33] But *spectral congestion* is very often cited as a common problem for its use[34,35] as was recently reported (for example) to separate resonances of a target molecule from a surrounding lipid matrix.[36] In the technique developed here, electrochemistry provides an external "switch" wherefrom variations in specific SERS signals can be introduced at will (and with a given periodicity). Fluctuation analysis with methods like principal component analysis (PCA)—either by itself or assisted by Fourier "lock-in" prefiltering (vide infra)—can easily follow from here, thus providing a systematic method to isolate SERS signals from different species along the electrochemical cycle (in the background of many possible, sometimes undesirable, contributions).

Electrochemical modulation and signal discrimination could become a very important tool in areas like bioelectrochemistry, to isolate the signals from different species in redox active sites, in samples where we cannot choose at will the purity or spectral characteristics of all the components. The situation of overlapping peaks—or much larger signals from spurious molecules—can prevent the isolation of the interesting spectra displaying an oxidation/reduction cycle. Therefore, the technique is aimed at applications in this latter case, and it applies particularly well to address cases of *coadsorption*; which is a classic case applicable to the electrochemistry of complex multicomponent systems (like biological systems).

EXPERIMENTAL SECTION

A three-electrode cell with a Ag/AgCl (1 M Cl^-) electrode and a high-area platinum foil as reference and counter electrodes, respectively, was used. The working electrode (see below for further details) is immersed in the electrolyte solution (phosphate buffer, pH 6) and this is placed inside an open electrochemical cell that allows focusing on the substrate with long working distance objectives (×10, ×20, ×50, or ×100) through a water/air interface (see the Supporting Information (SI) for further details). All the potentials reported here are referenced to the Ag/AgCl (1 M Cl^-) electrode. Cyclic voltammetry is performed with a potentiostat with digital data acquisition. The whole assembly is placed on top of a motorized $x-y$ stage for microscopy (to allow exploration and mapping of the electrode) and is used on a BX41 Olympus microscope attached to a Jobin-Yvon LabRam spectrometer. All the experiments performed in this paper are done with the 633 nm line of a HeNe laser with 3 mW at the sample. For samples with "high" concentrations of dyes (for SERS standards) like ~20−40 nM, we are mainly interested in *average* signals over the substrate. Therefore, we typically use for these experiments

(21) Ward, D. R.; Halas, N. J.; Ciszek, J. W.; Tour, J. M.; Wu, Y.; Nordlander, P.; Natelson, D. *Nano Lett.* **2008**, *8*, 919–924.
(22) Lacharmoise, P. D.; Etchegoin, P. G.; Le Ru, E. C. *ACS Nano* **2009**, *3*, 66–72.
(23) Tian, Z. Q.; Li, W. H.; Mao, B. W.; Zou, S. Z.; Gao, J. S. *Appl. Spectrosc.* **1996**, *50*, 1569.
(24) Shi, C.; Zhang, W.; Birke, R. L.; Lombardi, J. R. *J. Phys. Chem.* **1990**, *94*, 4766–4769.
(25) Shan, X.; Patel, U.; Wang, S.; Iglesias, R.; Tao, N. *Science* **2010**, *327*, 1363–1366.
(26) Huang, B.; Yu, F.; Zare, R. N. *Anal. Chem.* **2007**, *79*, 2979–2983.
(27) Wang, S.; Huang, X.; Shan, X.; Foley, K. J.; Tao, N. *Anal. Chem.* **2010**, *82*, 935–941.
(28) Yu, P. Y.; Cardona, M. *Fundamentals of Semiconductors: Physics and Materials Properties*; Springer: Berlin, 2004.
(29) Scodeller, P.; Flexer, V.; Szamocki, R.; Calvo, E. J.; Tognalli, N.; Troiani, H.; Fainstein, A. *J. Am. Chem. Soc.* **2008**, *130*, 12690–12697.
(30) Daza Millone, M. A.; Vela, M. E.; Salvarezza, R. C.; Creczynski-Pasa, T. B.; Tognalli, N. G.; Fainstein, A. *Chem. Phys. Chem.* **2009**, *10*, 1927–1933.
(31) Tognalli, N. G.; Fainstein, A.; Vericat, C.; Vela, M. E.; Salvarezza, R. C. *J. Phys. Chem. C* **2008**, *112*, 3741–3746.
(32) Kranich, A.; Naumann, H.; Molina-Heredia, F. P.; Moore, H. J.; Lee, T. R.; Lecomte, S.; de la Rosa, M. A.; Hildebrandt, P.; Murgida, D. H. *Phys. Chem. Chem. Phys.* **2009**, *11*, 7390–7397.
(33) Etchegoin, P. G.; Van Duyne, R. P. *Phys. Chem. Chem. Phys.* **2008**, *10*, 6079.
(34) Casadio, F.; Leona, M.; Lombardi, J. R.; Van Duyne, R. P. *Acc. Chem. Res.* **2010**, *43*, 782–791.
(35) Golightly, R. S.; Doering, W. E.; Natan, M. J. *ACS nano* **2009**, *3*, 2859–2869.
(36) Nguyen, T. T.; Rembert, K.; Conboy, J. C. *J. Am. Chem. Soc.* **2009**, *131*, 1401–1403.

the ×10 objective, to have a large spot diameter ∼10 μm, and minimize photobleaching effects as much as possible.

Rhodamine 6G (RH6G), nile blue (NB), and crystal violet (CV) were obtained from commercial sources (Aldrich) and mixed at the appropriate concentrations with borohydride-reduced Ag colloids[37] (to avoid a citrate capping layer) and with 20 mM KCl; to induce a slight destabilization and the formation of clusters.[38] For each case reported here, the details about the specific concentrations being used are specified in the captions. RH6G, NB, and CV adsorb to the negatively-charged colloids in this case through electrostatic interactions. The colloidal solution is subsequently drop-casted and dried under a mild heat on a clean Ag foil. Once dried, the colloids stick to the Ag foil by van der Waals forces, and remain attached to it upon reimmersion in the phosphate buffer solution. Several regions with multiple dried clusters of colloids can be easily distinguished in the microscope image on the Ag surface after drying. Hence, the Ag foil with the colloids and the dyes is our working electrode, and also provides the ideal means whereupon SERS enhancements (to observe low dye concentrations) can coexists with the ability to perform electrochemistry on the attached molecules. We checked at much higher concentrations (∼1 mM) that, as far the voltamperogram is concerned, the electrochemistry of the dyes on the colloids is indistinguishable from the one where the dyes are directly attached to the Ag foil itself. Note also that, in all of the experiments performed in this work, the dyes were adsorbed beforehand on the colloids (i.e., the dyes are not dissolved in the electrolyte solution itself).

ELECTROCHEMICAL MODULATION AND SIGNAL ISOLATION

Mixture of NB and RH6G. To fix ideas, we develop the method through an example. Consider the case of a mixture of two classic SERS dyes: RH6G and NB in concentrations of 40 and 20 nM, respectively. We perform cyclic voltammetric runs varying the scan rate (i.e., the period), typically in the range ∼20−100 s per cycle, while monitoring the SERS signal on the electrode simultaneously with a much smaller integration time to follow the dynamics. This gives us the possibility to choose the best scan rate that allows us to follow the dynamics of the system. According also to the choice of the potential window, the different coadsorbed species will be modulated differently. This adds then a second degree of freedom (besides the period of the modulation) to be chosen by the experimentalist: that is, the potential range of the modulation. In the case of Figure 1 we modulated the potential in the range between −50 and −550 mV at a fix scan rate of 50 mV·sec^{-1}. NB will experience oxidation/reduction cycles between these two values, while RH6G will only start to be reduced at a potential of ∼−400 mV and lower.[17] Another important detail is that the electrochemical modulation does not cross at any point the *potential of zero charge* (pzc = −0.9 V) of the electrode,[39] meaning that the dyes (which are positively charged in solution) remain all the time on a positively charged electrode in the entire modulation range. None of the phenomena reported in this paper can be ascribed to adsorption/desorption produced by a change in polarity of the electrode across the pzc point, but rather to oxidation/reduction of the species. Note also that the scan rates used in our experiences are fast enough compared to those reported for "electrostatic guiding".[17,22]

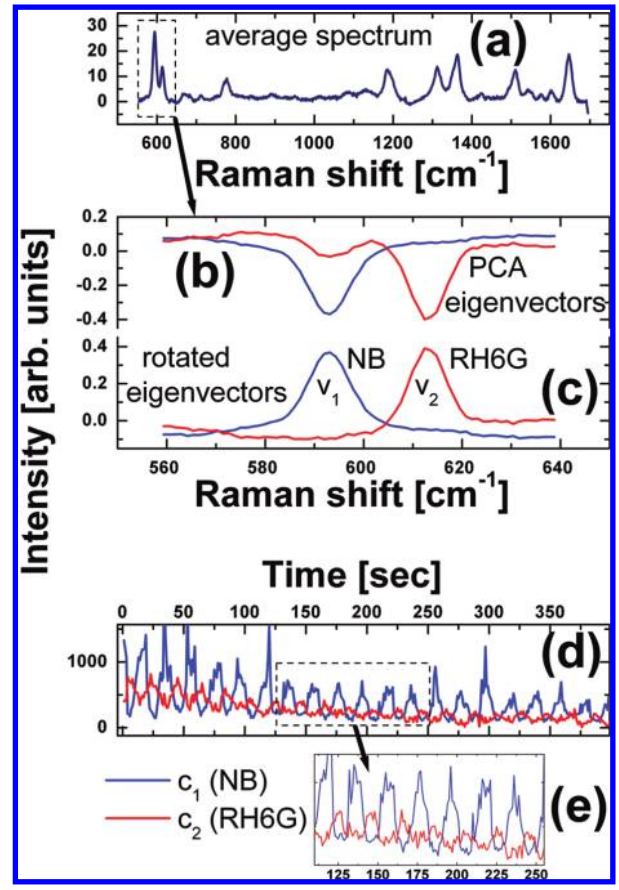

Figure 1. (a) Average spectrum for a sample with 20 nM of NB and 40 nM of RH6G which is modulated electrochemically in the potential range −50 to −550 mV at a scan rate of 50 mV·sec^{-1}. Both signals of NB and RH6G are clearly visible, and both dyes are modulated in different electrochemical potential ranges. The "fingerprint" region containing the 590 cm^{-1} mode of NB and the 610 cm^{-1} one of RH6G (dashed box in (a)) is analyzed by PCA, resulting in the two dominant eigenvectors shown in (b). The spectra in (b) contains a *linear combination* of the two independent spectra of NB and RH6G, which can be obtained by a suitable change of basis (described in full detail in ref 40). The new eigenvectors (obtained from a linear combination of the PCA ones) that describe the two physically independent components (NB and RH6G) are shown in (c). With these eigenvectors we can make a decomposition of the spectra to obtain the two coefficients that describe (for each event) the intensity as a linear combination of v_1 and v_2. These coefficients are shown in (d), with a blown-out region in (e) where the dephasing of the electrochemical modulation of both signals can be observed.

In order to optimize the presentation of the material here without dwelling too much into collateral issues, we present the main details of the basic electrochemistry of NB and RH6G in the SI, as well as the basic aspects of the analysis with principal component analysis (PCA), and PCA with FFT prefiltering.[41,42] As explained in the SI, both analysis techniques (PCA and FFT) are quite widespread, and we shall therefore assume that the

(37) Creighton, J. A.; Blatchford, C. G.; Albrecht, M. G. *J. Chem. Soc., Faraday Trans. 2* **1979**, *75*, 790–798.
(38) Meyer, M.; Le Ru, E. C.; Etchegoin, P. G. *J. Phys. Chem. B* **2006**, *110*, 6040.
(39) Niaura, G.; Gaigalas, A. K.; Vilker, V. L. *J. Phys. Chem. B* **1997**, *101*, 9250–9262.

reader has a basic understanding of them. Hereafter, we shall go directly to the presentation of the main results.

Figure 1(a) shows the average signal over 400 spectra taken with integration time of 1 s, with an electrochemical modulation period of 20 s. The average has clear fingerprint peaks of both dyes; for example the 590 and 610 cm^{-1} modes of NB and RH6G, respectively. The intensity of these peaks is modulated differently in the potential window selected, that is, their redox potentials are different. This is a case nevertheless where both signals of the coadsorbed species are clearly visible, and show in some cases some degree of overlap (like the 1645 and 1650 cm^{-1} modes of NB and RH6G, respectively). We first show an analysis in Figure 1 based on a spectral region that contains fingerprint modes of both dyes, like the region around ~600 cm^{-1} shown in a dashed box in Figure 1(a). A PCA analysis of this region[40] immediately identifies the presence of two main modulated components in the spectra. As explained in the SI though, being a linear decomposition technique, PCA always provides a *linear combination* of the right answer in the form of principal "eigenvector" spectra (in this case the first two of them, shown in Figure 1(b)). In order to go from this two PCA eigenvectors to the real spectra that represent the individual contributions of NB and RH6G, a linear transformation (which we shall call "rotation") of these eigenvectors is required. An entirely equivalent situation occurs with the application of PCA to the analysis of fluctuations from single molecule spectra; as explained in full length in ref 40. The "rotated" eigenvectors obtained in this case are shown in Figure 1(c), and represent the isolated contributions of NB and RH6G to each individual spectrum. Once these two eigenvector spectra (v_1 and v_2 in Figure 1(c)) are known, a standard linear decomposition can be performed on each spectra I_i in the time series ($i = 1, 2, ..., 400$), to represent it as a linear combination (with two coefficients) of the rotated PCA eigenvectors; that is, $I_i = c_1v_1 + c_2v_2$. The values of the coefficients, therefore, represent the particular contribution of NB and RH6G to an individual spectrum, and this is shown explicitly in Figure 1(d). Figure 1(e), in addition, shows a blown-out region of the time evolution of the coefficients where it can be appreciated that the two signals are being modulated differently at different times, accounting for the different intrinsic electrochemical properties of both dyes as a function of the sweeping potential. Note that time evolution can be converted to potential, since we know exactly the period of electrochemical modulation applied externally. An example of this is shown in the SI. The coefficients in Figure 1(d) and (e) are obviously in arbitrary units, since the Raman intensity itself is in arbitrary units too. What matters is not the absolute units, but rather the relative values of the coefficients representing the particular contributions to the total coming from the different electrochemical species.

Therefore, Figure 1 demonstrates clearly that the combination of electrochemical modulation with PCA analysis can (i) resolve the problem of spectral congestion, and (ii) identify in addition the ranges of electrochemical potentials where the different species experience their modulation. This is emphasized in Figure 1(e), where the "dephasing" of the coefficients c_1 and c_2 representing the relative contributions of NB and RH6G, respectively, can be easily seen. The fact that RH6G only starts to be reduced toward the lowest negative range of the potential ($E < -400$ mV) appears as a "dephasing" of the coefficients in time, while the successive electrochemical cycles evolve. Figure 1(d) also shows a slight reduction in the amplitude of the coefficients produced by photobleaching at the observation point. It may also have partial contribution from natural long-term desorption of the dyes into the buffer. Photobleaching, in general, tends to be one of the major limiting factors to obtain unlimited sampling of the signal.

Moving on from the simplest case in Figure 1, if we want to carry out the analysis over the entire spectral range (rather than a small window with fingerprint modes, like in Figure 1), special care must be taken with background contributions. Backgrounds are in general problematic in SERS[43] and, unlike the Raman peaks themselves, they can have a variety of origins (including molecules that are not in contact with the electrode). Furthermore, there will be in general a correlation between the background and the Raman signal created by the dispersion of the plasmon resonances producing SERS.[43−45] Here, we want to concentrate in a first approximation only on the Raman signals themselves and, therefore, the background will be removed[46] to avoid its presence in the PCA analysis. This should be done with care and the results should be assessed on a case-by-case basis. Backgrounds in SERS can be particularly problematic in the single molecule limit, where the dispersion of an individual plasmon resonance at a hot-spot can be revealed.[43,47] Measuring an average over many molecules is in a way an advantage, for differing types of backgrounds tend to average out and we are left with a case of background contribution that is easier to subtract. The background of each individual spectrum is subtracted with a wavelet transform that is fully described in ref 46 (including the program which is freely available[46]). The success of the background subtraction procedure to deconvolute the spectra is judged here by the ability of the PCA analysis to distinguish the two main contributions to the signal in the full spectral range (which are known in this case).

Effectively, Figure 2 shows the equivalent analysis of Figure 1 in the full spectral range. Once the backgrounds are subtracted, and the two main PCA eigenvector spectra rotated, we recover the independent spectra of NB and RH6G from the mixture. Except for a few minor imperfections, the separation of the spectral components is almost perfect, and can be also distinguished in terms of the respective electrochemical modulation ranges for the potential. As in Figures 1(d) and (e), the dephasing of the coefficients from the contributions of NB and RH6G, according to the different values of the redox potentials over the cyclic voltammetry runs, can be clearly observed again in Figure 2(d). It is particularly worth emphasizing that the spectral deconvolution

(40) Etchegoin, P. G.; Meyer, M.; Blackie, E.; Le Ru, E. C. *Anal. Chem.* **2007**, *79*, 8411.
(41) Jolliffe, I. T. *Principal Component Analysis*; Springer Verlag:Berlin, 2002.
(42) Hyvrinen, A.; Karhunen, J.; Oja, E. *Independent Component Analysis*; John Wiley & Sons: New York, 2001.
(43) Buchanan, S.; Le Ru, E. C.; Etchegoin, P. G. *Phys. Chem. Chem. Phys.* **2009**, *11*, 7406.
(44) Le Ru, E. C.; Etchegoin, P. G.; Grand, J.; Felidj, N.; Aubard, J.; Levi, G.; Hohenau, A.; Krenn, J. R. *Curr. Appl. Phys.* **2008**, *8*, 467.
(45) Le Ru, E. C.; Grand, J.; Felidj, N.; Aubard, J.; Levi, G.; Hohenau, A.; Krenn, J. R.; Blackie, E.; Etchegoin, P. G. *J. Phys. Chem. C* **2008**, *112*, 8117.
(46) Galloway, C.; Le Ru, E. C.; Etchegoin, P. G. *Appl. Spectrosc.* **2009**, *63*, 1371.
(47) Itoh, T.; Yoshida, K.; Biju, V.; Kikkawa, Y.; Ishikawa, M.; Ozaki, Y. *Phys. Rev. B* **2007**, *76*, 085405.

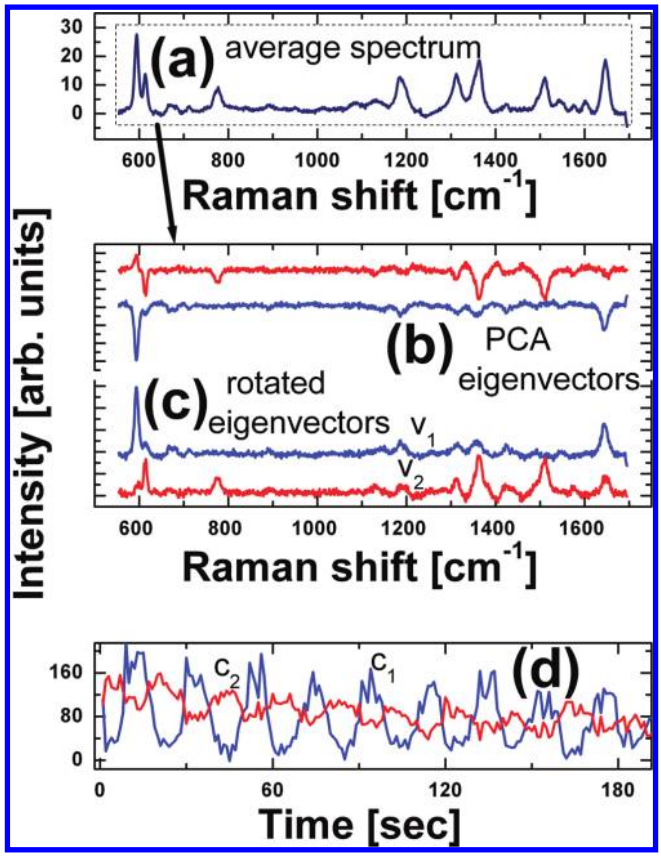

Figure 2. With a suitable removal of the background[46] for all events, the full spectra of NB and RH6G can be deconvoluted again from the modulated time series through PCA. The region analyzed now is the full spectral window shown in (a) (dashed line). The two main eigenvectors and the "rotated" ones[40] (representing the independent contributions of NB and RH6G) are shown in (b) and (c), respectively. The spectra of two compounds can be deconvoluted, and their time (or potential) dependence followed through the time evolution of the two coefficients in (d), that describe each event as a linear combination of v_1 and v_2 in (c). The dephasing of the electrochemical modulation of the two compounds can again be appreciated in (d).

through the electrochemical modulation works very well even in regions where a substantial overlap of peaks occurs. An example of the latter is shown in Figure 3, for the region around ~1650 cm^{-1}, which has contributions from breathing modes of both NB and RH6G (but at slightly different frequencies). As can be appreciated from Figure 3, the different modulation induced through the electrochemical cycle on both compounds is good enough to "deconvolute" closely laying peaks within their natural widths.

Mixture of NB and CV. All in all, the case presented in the previous section represents a relative "easy" case of spectral deconvolution for PCA with electrochemical modulation; starting from the fact that both compounds have comparable contributions to the intensity of the spectra and can be easily identified in terms of their contributions to fluctuations (which is the whole basis of PCA[41,42]). A substantially more challenging case is to try recover a small signal from a background of other contributions to the spectra (that might be unavoidable in many real cases). We treat this case here also with an example.

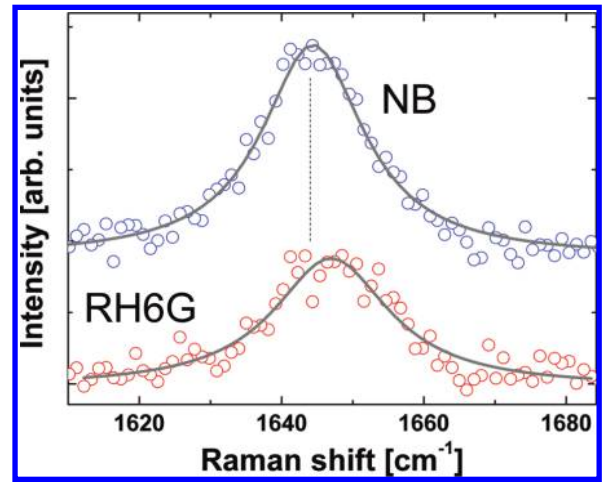

Figure 3. The deconvolution of the spectra works even in regions where there is a substantial overlap of peak intensities for the different compounds. Here we show explicitly the region ~1650 cm^{-1}, where the RH6G peak is deconvoluted from the equivalent ring-breathing mode in NB, which is at a slightly lower frequency.

Consider the case of a mixture of 80 and 20 nM of CV and NB, respectively, as shown in Figure 4(a). The mixture is prepared purposely so that the signal of NB is barely visible in the average spectrum (Figure 1(a)). This is shown explicitly, for example, with the arrows pointing at the ~590 and ~1650 cm^{-1} fingerprint peaks of NB in Figure 4(a), which are almost buried in the immediate surrounding of much larger peaks from CV. Both NB and CV experience (different) electrochemical modulations in the potential range between −50 and −550 mV (the electrochemistry of CV is also summarized in the SI). We can basically follow in a first approximation the analysis performed in the previous section.

With an unlimited amount of sampling, PCA has all what it needs to distinguish the different components in the spectra. This is because the eigenvalues and eigenvectors of the covariance matrix (which is the basis of PCA[41,42]) will eventually distinguish what is correlated and what is random in the signal. For the same reason that unlimited integration time should in principle always lift a signal above the noise level, sufficient sampling will always provide PCA with all the information required to distinguish the different contributions to the spectra. Nevertheless, when big signals are mixed with very small ones from other independent contributions, it is the comparative (with respect to other larger signals in the spectrum) size of the small signals that fix the amount of sampling we need to obtain the principal components from the spectra. This amount of sampling can be, however, prohibitively large. In the case of SERS, for example, photobleaching and other long-term stability problems of the signal puts serious limitation to how much sampling we can obtain. We are left here basically with a conundrum: random fluctuations in large signals with limited sampling might be comparable—as far as contributions to the covariance matrix of PCA is concerned—to the small signals we are trying to modulate and detect on purpose. An example of this is explicitly shown in Figure 4; the region encircled in a box in Figure 4(a) contains a contribution from NB and a much larger peak of CV in the same range. This region is PCA-analyzed and the first four eigenvectors are shown in Figure 4(b). We can see that there is no clear signature of the NB peak in the PCA analysis. The first eigenvector is clearly dominated

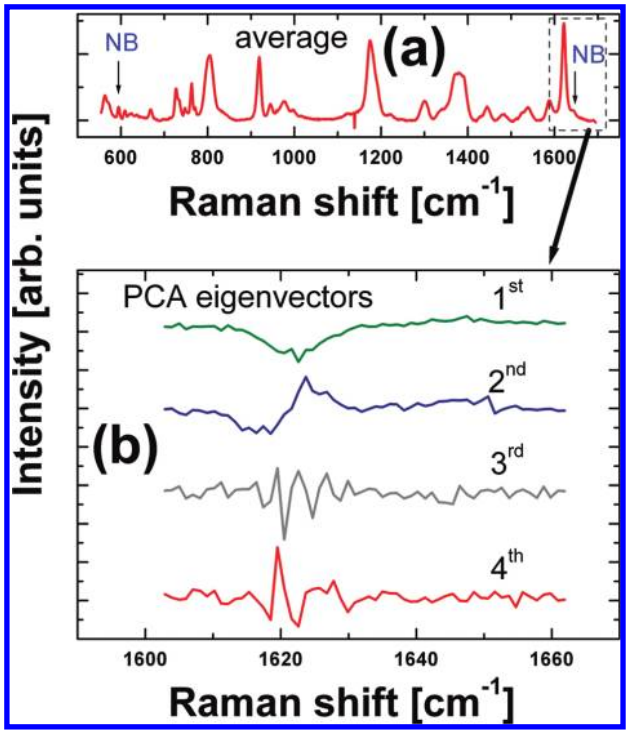

Figure 4. With limited sampling, PCA can have problems to distinguish small components in the spectra. An example is shown here with a mixture of 80 and 20 nM of CV and NB, respectively. In (a) we show the average (over 400 spectra), with arrows showing the positions where the fingerprint modes of NB at 590 cm^{-1} and 1645 cm^{-1} should appear. The signal is dominated by CV throughout the entire spectral range, with many overlap regions. In (b) we show a PCA analysis of the ~1630 cm^{-1} region, where both the 1620 and 1645 cm^{-1} peaks of CV and NB are expected, respectively. But with a difference of factor of ~20 between the intensities of CV and NB in this range, fluctuations larger than ~5% in the CV signal have a larger weight for the covariance matrix than the induced (electrochemical) variations of NB. With limited sampling, PCA cannot clearly distinguish the NB signal. We show here the first four PCA eigenvectors as an example. The limited sampling problem can be partially compensated by a prefiltering of the data with a FFT-transform, filtered at the appropriate electrochemical modulation frequency (see Figure 5).

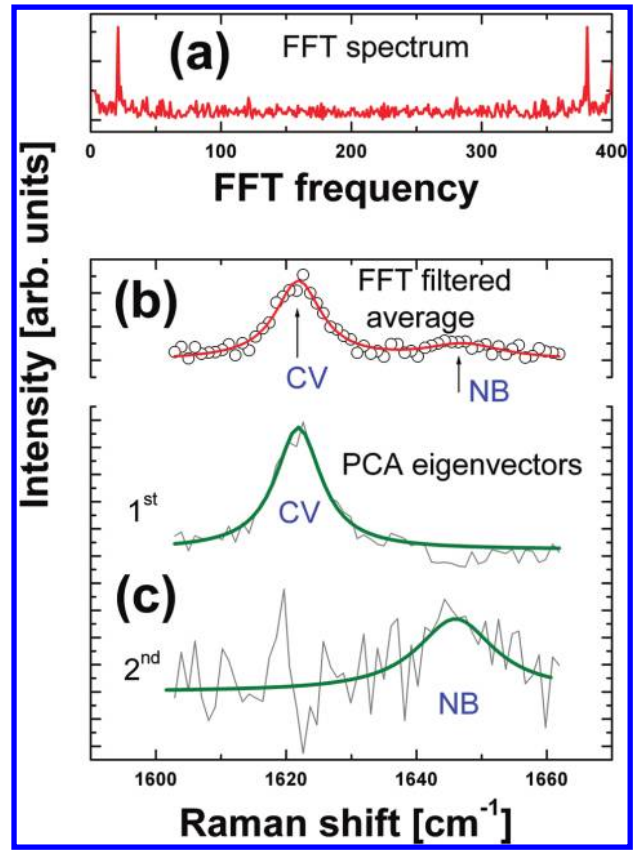

Figure 5. (a) A FFT of the total integrated intensity of the spectra (which varies mainly here due to the electrochemical modulation of CV), reveals clearly the main frequency of the modulation (i.e., scan rate of 50 mV. sec^{-1}). We can filter each pixel (wavelength) at this frequency and then transformed back the spectra into the time domain. The average of the filtered data (at the electrochemical modulation frequency) is shown in (b). Now the signal of NB is more clearly visible in the average and its relative intensity with respect to the CV peak is larger (because only the part of the CV signal that is modulated survives the filtering). A PCA analysis of the prefiltered signal shows a first eigenvector representing the CV intensity, and a second eigenvector which now contains the NB peak at ~1645 cm^{-1}, and a small fraction of frequency shifts of the CV peak. The vertical intensity scale for both curves in (c) is the same. Green lines are guides to the eye.

by the intensity fluctuations of the much larger CV peak, whereas the second one has the typical characteristic of an eigenvector accounting for *frequency shifts* of the CV peak.[40] From the third eigenvector onward, the covariance matrix in PCA is trying to find "correlations in the noise". With enough sampling, these correlations will be zero and the peak of NB will appear as a third eigenvector. But in this case, the limited sampling establishes a competition between the random fluctuations of the much larger peak and the signal we are trying to observe (from NB).

It is in situations like this one that a prefiltering of the data can help. The basic idea of Fourier prefiltering is explained in full in the SI with further examples, but here we shall give a brief version of it. From a FFT-transform of the total integrated intensity as a function of time we can easily reveal the main modulation frequency in the FFT-spectrum, as can be seen in Figure 5(a). This comes primarily from the modulation of the CV signal, but that is irrelevant at this stage: the FFT-transform of the total integrated intensity is used to identify the modulation in FFT-frequency units.[48−50] We can now perform a wavelength-by-wavelength (i.e., pixel-by-pixel) FFT filtering of the data at this particular frequency. This is simply done by an FFT-transform to the time evolution of each pixel, multiplication by an appropriate filter centered at the spikes of Figure 5(a), and followed by an inverse FFT-transform to go back to the time domain. In these data, therefore, we have enhanced the importance of only those fluctuations that happen at the known electrochemical modulation frequency, with respect to any other random fluctuation.

Figure 5(b) and (c) show the resulting PCA analysis after FFT-filtering. It is worth noting that the average of the filtered signal has now a much better ratio of intensities between the CV and NB signals; this is because only the fraction of the CV signal that is being modulated survives the filtering. Accordingly, this puts

(48) Press, W. H.; Flannery, B. P.; Teukolsky, S. A.; Vetterling, W. T. *Numerical Recipes in FORTRAN: The Art of Scientific Computing*; Cambridge University Press: Cambridge, 1989.
(49) Kreyszig, E. *Advanced Engineering Mathematics*, 9th ed.; John Wiley & Sons: New York, 2006.
(50) Kauppinen, J.; Partanen, J. *Fourier Transforms in Spectroscopy*; Wiley-VCH Verlag: Berlin, 2001.

the NB signal in a much better footing to be identified among the first PCA eigenvectors. Effectively, we can see now in Figure 5(c) that the first eigenvector is still dominated by the CV signal, but the second one contains both the NB signal and some contributions to frequency shifts of the CV peak. What we have achieved by FFT-prefiltering is to put the NB signal at the same level of importance of frequency shifts of the CV peak (according to the covariance matrix) and this therefore "lifts" a very small signal from accidental correlations in the noise. As explained further in the SI, this is nothing but the well established principle of "lock-in" amplification; applied here as a prefiltering for PCA. In general, in any other experimental situation, if we have access to unlimited sampling then time lock-in "amplification" might not be needed; for the signal will always increase linearly with time while the noise increases like the square root of it. Therefore, the signal-to-noise ratio will always improve with integration time and eventually a small signal can be resolved. But we can achieve a much faster result in a shorter time (with less sampling) with a lock-in. Like in the case at hand here, unlimited amount of sampling is sometimes not possible in other experimental situations because the long-term stability of the experiment is compromised or it is simply too long. The situation depicted here is the exact analog of this latter situation but for the problem of spectral deconvolution with PCA.

The combination of FFT-prefiltering and PCA might not be necessary in many situations and whenever possible, the simplest analysis should prevail. But the covariance matrix of PCA is basically "blind" to the time sequence of the electrochemical cycle. If we scrambled all the spectra (in time) we would still have the same covariance matrix and the same PCA eigenvectors. However, we *do* know the frequency (or period) with which we are inducing the electrochemical modulation. What we are doing with FFT-prefiltering is, accordingly, to "pick" the appropriate fluctuations that happen at the frequency where we know the real physical effect is happening. In that manner, we bias the PCA analysis toward a physically relevant set of fluctuations, and this helps to improve the ability of PCA to distinguish what is correlated and what is not, in a situation where limited sampling is unavoidable. In the language of lock-in amplification, we have improved the signal-to-noise ratio by discarding all fluctuations except those that happen at the right frequency. The example chosen here is tailor-made to show the concept and, as such, we have different options at hand. We could have done, for example, a PCA analysis is a much narrower window around the NB peak (to try to minimize the influence of the CV peak nearby). However, in real applications, we might not even know where to expect the peaks, and considerable spectral overlap is always possible. FFT-prefiltering is one additional tool to consider in these situation, and it could -in many cases- be the difference between being able to isolate a particular spectral feature of the weaker signal or not.

CONCLUSIONS

We have shown a combination of electrochemical modulation with fluctuation analysis to discriminate and isolate different species in cases where there is spectral congestion and coadsorption of molecules. Needless to say, the technique is not limited to *two* species, and can be applied to multicomponent systems in general. PCA contains, in principle, all the elements it needs to distinguish all spectral components given enough sampling. The restriction of limited sampling to "lift" small signals from other contributions has also been shown through the addition of FFT-prefiltering. Prefiltering is not strange in PCA analysis. The most common type of prefiltering used in the PCA literature is "pre-whitening".[41,42] In this latter case, this is done for a different purpose: to ensure that the samples are as unbiased as possible before the PCA analysis is carried out. Here we use prefiltering in a different way: to bias the study of correlations in the data that happen at a prescribed frequency, imposed externally by the electrochemical modulation. We believe that techniques to solve spectral congestion of coadsorbed species will be of great interest, as SERS moves into areas (like bioelectrochemistry) where the purity and characteristics of the sample cannot be chosen at will. We hope the concepts developed here in our paper will contribute to that endeavor.

ACKNOWLEDGMENT

E.C. acknowledges the financial support of UNLP, ANPCyT (Argentina) and the MacDiarmid Institute (New Zealand) for a research/exchange program between Argentina and New Zealand. Thanks are also given to the host institution, Victoria University of Wellington, where the work was carried out. We acknowledge financial support from ANPCyT (Argentina, PICT06-621, PAE 22711, PICT06-01061, PICT-CNPQ 08-019). E.C., A.F., and RCS are also at CONICET. MEV is a member of the research career of CIC BsAs. R.C.S and A.F. are Guggenheim Foundation Fellows. PGE and ECLR are indebted to the Royal Society of New Zealand for additional financial support under a Marsden Grant.

SUPPORTING INFORMATION AVAILABLE

Additional information and figures. This material is available free of charge via the Internet at http://pubs.acs.org.

Received for review May 3, 2010. Accepted July 10, 2010.

AC101152T

Supplementary information for "Electrochemical modulation for signal discrimination in Surface Enhanced Raman Scattering (SERS)"

Emiliano Cortés, Pablo G. Etchegoin, Eric C. Le Ru, Alejandro Fainstein, María E. Vela, and Roberto C. Salvarezza

SERS ELECTROCHEMISTRY OF NILE BLUE (NB)

The electrochemistry of Nile Blue (NB) and similar (related) dyes has been extensively studied in the past from both a purely electrochemical and/or SERS points of view [1–5]. In that sense (and unlike other common dyes used in SERS), the presence of copious previous experimental information facilitates here the explanation of the basic phenomenology of SERS of NB under standard electrochemical conditions. Nile Blue has a reduction/oxidation (redox) potential centered at $\sim -0.35\,\mathrm{V}$ on Ag (with respect to a Ag/AgCl reference electrode). The basic voltamperogram of NB measured in our cell is shown in Fig. S1.

The cell allows the simultaneous monitoring of the electrochemical cycle while the Raman (SERS) signal of the molecules on the Ag working electrode is followed. We can focus through an air/water interface with long working distance (LWD) ×10, ×20, ×50, or ×100 objectives (thus achieving different power densities on the electrode for a fixed incident laser power of $3\,\mathrm{mW}, \lambda = 633\,\mathrm{nm}$). The experimental layout is schematically shown in the inset of Fig. S1. Examples of SERS signals of NB in both the oxidized and reduced states are provided in Fig. S2(a), together with an example of the SERS signal following the electrochemical modulation in time. This "handle" on the intensity of the SERS signal of NB – which is controlled by the applied potential– is taken as the basis for the different methods proposed in the paper. The modulation is used to filter and isolate the different components in the spectra, either by means of Principal Component Analysis (PCA), Fourier filtering, or combinations thereof (see the last section for further details).

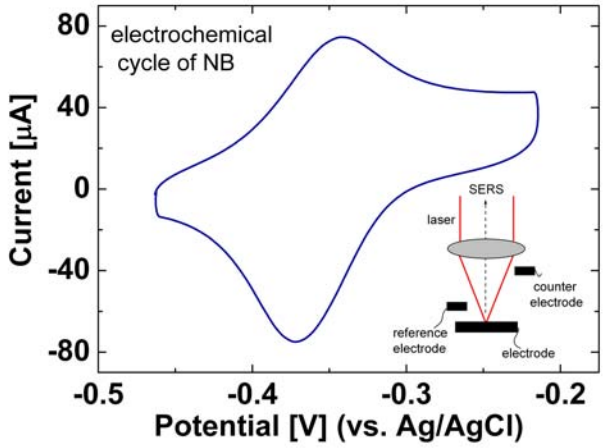

FIG. S1: Cyclic voltamperometry of NB on Ag in buffer phosphate (pH$\sim$ 6) recorded at $0.1\,\mathrm{V.s^{-1}}$ measured in our cell. The cell allows the simultaneous measurement of the electrochemical behavior of the molecules on the Ag working electrode and the SERS signals (inset). A large area Pt foil and a Ag/AgCl electrode were used as counter and reference electrodes respectively. NB undergoes oxidation/reduction transformations at $\sim -0.35\,\mathrm{V}$ resulting in a change in the intensity of SERS signals from the highly resonant oxidized state, to the non-resonant reduced one [1–5]. Examples of both cases are shown in Fig. S2(a).

SERS ELECTROCHEMISTRY OF RHODAMINE 6G (RH6G)

The electrochemistry of RH6G is more subtle and has not been studied as extensively as NB. While some papers concentrate mainly on the electrochemistry of RH6G affecting its fluorescent properties [6, 7], the information on SERS electrochemistry of RH6G is (comparatively speaking) almost inexistent. An exception to the rule is the recent paper by Brolo *et. al.* [8], where an electrochemical cell was used in combination with SERS to demonstrate the control of fluctuations coming from a small number of SERS-active molecules. In this latter case, the potential is not used as a way of inducing a redox transition, but mainly as an electrostatic way of sticking or detaching molecules from surfaces according to their intrinsic charge in solution; i.e. to control the adsorption/desorption dynamics [9]. RH6G reduction starts at potentials close to $\sim -0.4\,\mathrm{V}$ leading in small changes in absolute and relative intensities among Raman peaks, i.e. some molecules are already being reduced at that potential. Even though the objective here is *not* to analyze the electrochemistry of RH6G in any detail (for which there is not even a proper theoretical background, as there is for CV), it is important to know about the existence of these changes; for they are present in the data. Accordingly, the small electrochemical modulation of RH6G is a "secondary" effect in our experiments; one that we try to isolate and separate from the contributions of molecules that do have a "complete" redox transition in the modulation region (NB in our case).

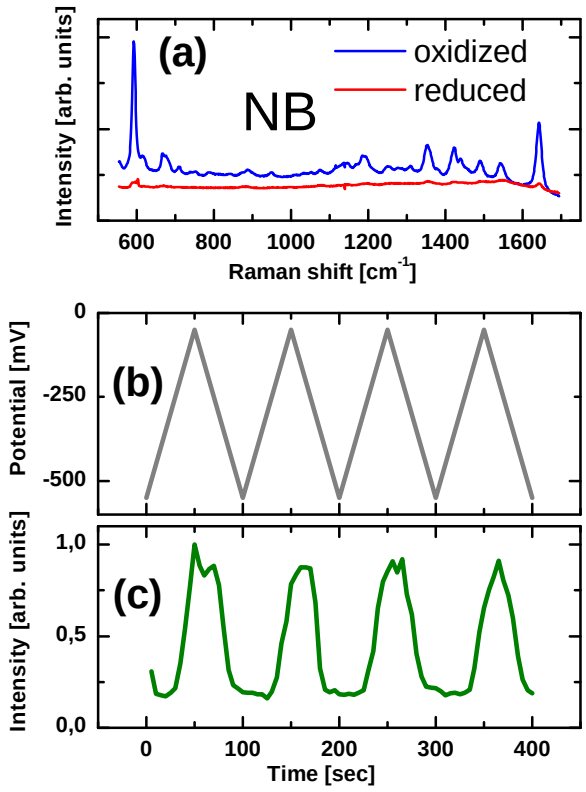

FIG. S2: (a) SERS spectra of NB at 633 nm laser excitation (3 mW, ×10 objective) in both the reduced ($V \sim -0.46$ V) and oxidized ($V \sim -0.21$ V) states on the Ag electrode. In (c) we show the continuous modulation of the SERS intensity of the $\sim 590\,\mathrm{cm}^{-1}$ mode of NB following the main frequency imposed by the alternate sweeping of the electrochemical potential (shown in (b)). This controlled intensity modulation is used as a basis for the discrimination of fluctuations by either PCA, Fourier analysis, or a combination thereof.

Brolo *et.at.* [8] also report that the electrochemical reduction of RH6G starts at ~ -0.4 V. From the SERS point of view, this results in a slight increase of the intensity in the average SERS spectrum of RH6G at 633 nm laser excitation. This is the opposite situation with respect to NB, meaning that the reduced state is slightly more resonant than the oxidized one at 633 nm. Furthermore, a PCA study of the SERS electrochemical modulation of RH6G (performed by us, in the potential window used in this work $-0.55\,\mathrm{V} < E < -0.05\,\mathrm{V}$) reveals that there are two main components to this modulation: one that accounts to the overall modulation of the intensity of all peaks, and a second component which accounts for small ($\sim 10\%$) *relative* changes of intensities among peaks. From the standpoint of having RH6G coadsorbed on the electrode with other species –that might show complete redox transitions in the chosen modulation range– the only relevant effect to account for is the overall modulation of the intensities of the peaks that will appear in RH6G if the modulation potential goes below ~ -0.4 V. Relative variations among peaks $\leq 10\%$ will play (if any) a secondary role. Still, any real application where RH6G is present will have to account for the overall (slight) modulation of the SERS intensity if the onset of charge transfer at ~ -0.4 V is surpassed in the modulation range of the electrochemical potential. This can become particularly important if the signal of RH6G dominates the spectrum while it is co-adsorbed with other species that might have either smaller concentrations, or weaker SERS cross sections. In this latter case, the *unwanted* modulation produced by a partial electrochemical reduction might become the "dominant" induced fluctuation in the data.

SERS ELECTROCHEMISTRY OF CRYSTAL VIOLET (CV)

As in the case of RH6G, the electrochemistry of crystal violet (CV) is somewhat subtler than that of NB. But unlike RH6G, the electrochemistry of CV has been previously studied in quite some detail [10–12]. There is evidence (both experimental and theoretical [11]) that CV experiences a certain degree of charge transfer as a function of the applied electrochemical potential (without resulting in an actual oxidation/reduction transformation). This degree of charge transfer has some measurable effects on some of the Raman bands detected in SERS. Reference [11], for example, is a comprehensive study (with Density Functional Theory, DFT) of the effects of the partial electrochemical charge transfer as a function of the applied potential for CV. There are very good reasons why CV has attracted more attention than RH6G for this type of studies. A theoretical study of partial charge transfer with DFT is greatly simplified in both its numerical implementation and in its interpretation if we can make effective use of *symmetry*. Accordingly, vibrations and electronic states can both be classified by their irreducible representations of a local point group, and the analysis of the effects of the partial charge transfer interaction is conceptually simpler (comparably speaking) and more amenable for DFT. On the other hand, the structure of RH6G can be broadly described by a three-ring chromophore (xanthene moiety) with a phenyl side-chain, which is in a different plane from the main backbone. The structure is by itself not as tractable in terms of exact symmetry classifications of vibrations and electronic states and, last but not least, the possible binding geometries and anchoring positions of RH6G on Ag are (in general) a lot more uncertain than for CV [13]. Hence, it naturally follows that a lot more is known and understood about partial electronic transfer in CV than in RH6G. In Ref. [11] it was found that the ~ 1592 and $1625\,\mathrm{cm}^{-1}$ Raman

bands of CV experience different degrees of charge transfer in the potential window used in this work to follow the NB redox couple ($-0.55\,\mathrm{V} > E > -0.05\,\mathrm{V}$). This results in a slight change of relative intensities of these bands as a function of electrochemical modulation. A brief summary of the situation for CV would be as follows: A partial charge transfer results in a (small) modulation of the SERS intensity, with some bands responding more than others according to their symmetry. There are, in fact, three different groups of bands according to Watanabe and Pettinger [10]. Still, these are effects that are not purely "redox" in nature and (as in the case of RH6G) we want to single them out and isolate them from the molecule we want to monitor (that experiences a complete oxidation/reduction transformation in the chosen potential range); which is NB in our case. Several different scenarios for this are discussed in further details in the next section.

PRINCIPAL COMPONENT ANALYSIS (PCA) VS. FOURIER FILTERING

In this section, we explain how Principal Component Analysis (PCA) and Fourier filtering apply to the different possible aspects of the same problem, i.e. the discrimination and isolation of SERS signals using electrochemical modulation. The two techniques can in many cases be applied independently of each other, and in most cases will provide similar (if not identical) results. In other cases, however, one technique outperforms the other and, moreover, they can sometimes be interwoven toward the goal of discriminating the contributions of the different species in a complex environment of signals.

Obviously, we cannot review all the principles of PCA [14, 15] and discrete Fourier analysis [16–18] here. However, being two of the most widespread analysis techniques used in spectroscopy and chemometrics, this is not a serious limitation here to analyze their different applications. It is assumed hereafter that the reader has a basic understanding of the basics of both PCA and Fast Fourier Transforms (FFT) [16–18]. There have been several applications of PCA to the analysis of SERS data in recent times [8], and a partial summary of the basic aspects can be found also in the supplementary information of Ref. [19]. Last, but not least, we shall avoid presenting the problem in its full general case for data analysis, but rather concentrate on specific examples relevant for our purposes here. In fact, we shall present the different aspects of the problem through a working example. This is done in the next subsection.

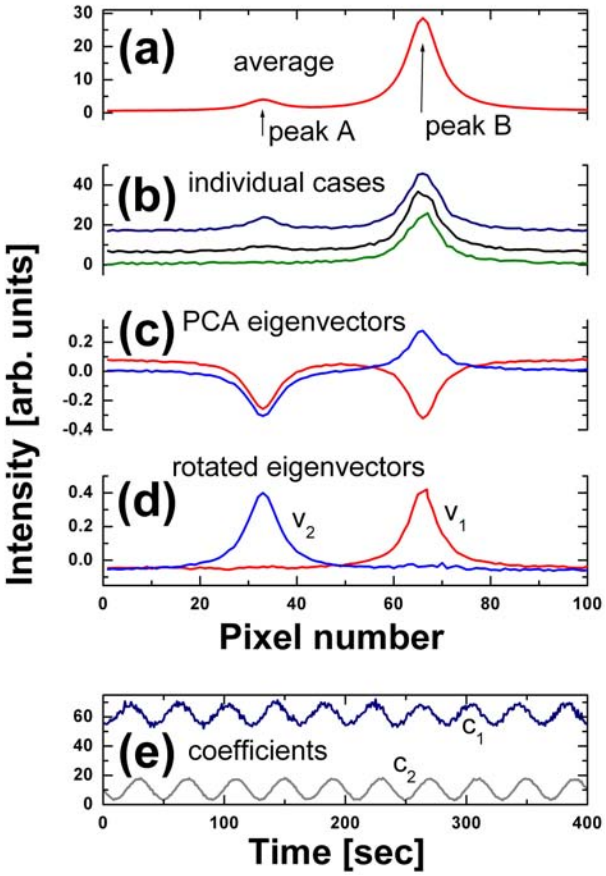

FIG. S3: Modeling of a spectral (CCD-pixel) range (of 100 pixels) with two peaks from two different hypothetical compounds: A; which experiences a full oxidation/reduction modulation in intensity (like NB), and B; which experiences only a 20% intensity modulation due to a partial charge transfer interaction (like RH6G or CV). There is also an arbitrary "dephasing" in time between the modulation of both intensities (as it would happen in many real situations). Both peaks (A and B) can be clearly distinguished in the average spectrum in (a) (over 400 simulated spectra) and in individual cases; three of which are shown in (b) (except when A is in the reduced state, in which case it does not show in that particular spectrum). The significant contributions to the fluctuations of the signal –above the added random fluctuations– of A and B implies that PCA clearly distinguishes both as independent components. The 1st and 2nd PCA eigenvectors in (c) contain already a linear combination of the two main spectra which, upon "rotation" to a new basis [19] results in the eigenvectors shwon in (d). A linear decomposition of the spectra in the eigenvectors in (d) results in the coefficient shown in (e). The largest part of the signal is contributed by v_1 with a coefficient c_1 that oscillates in time, and a smaller contribution (which sometimes reaches zero) comes from v_2 with coefficient c_2. The two contributions have a lag in time; which represents the different thresholds of the redox potential for A, and the onset of partial charge transfer for B. In this manner, all the intervening components and their dynamics have been isolated by PCA in this case.

Different applications of PCA and FFT

Suppose we have a spectral region with signal contributions from two different compounds: A and B. Suppose, for example, that there is a spectral region like that shown in S3 (which is plotted as intensity vs. pixel position on the CCD) where there are two peaks; one from compound A, and one from a co-adsorbed compound B. Furthermore, assume that the electrochemical modulation affects peak A through an oxidation/reduction cycle that results in a SERS signal for the oxidized state, and no signal for the reduced one. Like in the case of Nile Blue (NB), we shall assume that the main effect of going from the oxidized to the reduced state is in the *intensity* of peak A (due to a change in resonance condition). Accordingly, we have a 'handle" to modulate the fluctuations of peak A with a specified period T; assumed to be much larger than the sampling time per spectrum (integration time, τ). On the other hand, let us assume that peak B is only slightly modulated by the electrochemical cycle due to a partial charge transfer mechanism (like RH6G or CV). We shall assume, furthermore, that the onset potential of charge transfer for B and oxidation/reduction for A are not necessarily the same (i.e. they will appear at different potentials/times along the electrochemical cycle). There are two completely different situations for this problem depending on the relative intensity of the peaks and how the induced fluctuations in the signal of A compare to other underlying (uncontrolled) fluctuations in the system. Some of the limiting cases are relatively obvious and we therefore describe them briefly.

If the Raman signal of A is large enough (comparable to that of B), the induced variations in the signal of A constitute an important (and dominant) part of the fluctuations of the spectra; dominating over other (mostly uncontrollable) random fluctuations in the signal. This case is easily picked up by PCA [14, 15], which then – in general– not only allows the clear identification of the fluctuations of both compounds, but also provides all the different components of the spectra. This is fully summarized in Fig. S3.

Notwithstanding, even in this relatively easy case, several points need to be stressed. Being a *linear decomposition* problem, PCA will always give a 'linear combination of the right answer"; i.e. the two spectra that are picked up as the most important "eigenvectors" in the PCA decomposition will contain (in general) part of the signal of A and B. This is a well known (and unavoidable) feature of PCA that has been studied in full in Ref. [19], and requires basically a *rotation* of the vectors to create two spectra for the linear decomposition that are physically meaningful. This aspect is (in principle) automatically accounted for in techniques like Independent Component Analysis (ICA) –rather than PCA [14, 15]– but ICA works best for situation where the fluctuations are Gaussian-distributed [15], which is very often not the case in SERS data [19] and can lead to spurious or unphysical results. Very frequently, it is best to resolve the linear combination of PCA eigenvectors that give physically meaningful descriptions by a suitable rotation of the first two, and this is the procedure we chose here in Fig. S3.

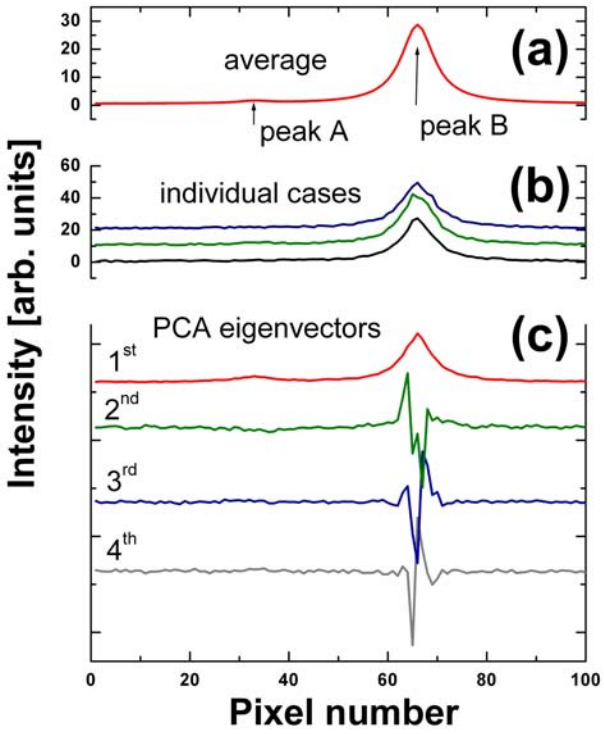

FIG. S4: A similar simulation to that in Fig. S3 but for a situation where peak A is *much* weaker than B. In this case, peak A is barely seen in the average spectrum (in (a)) and it is almost impossible to see in individual spectra; like the three examples shown in (b). A plain PCA analysis (shown in (c)) fails to easily identify the presence of peak A as an independent contribution to the fluctuations of the signal. There is a hint of the presence of peak A in the first PCA eigenvector, but all the higher order ones (shown up the 4^{th} here) concentrate on the random fluctuations of peak B. As far as contributions to the variance of the signal is concerned, the random fluctuations of peak B play a more dominant role than the *induced fluctuations* of peak A. The modulation of peak A is competing with larger fluctuations that do not allow its clear identification. The signal of A, however, can be "lifted" by a FFT pre-filtering, as shown in Fig. S5.

A more complicated situations arises if we are trying to recover a small signal coming from A in the presence of B. This is illustrated in Fig. S4. The problem here (as explained in the main paper) is that PCA does not discriminate fluctuations in terms of their physical importance, but only in terms of their magnitude. If A

is small and we can turn the signal on and off, we are inducing a well known fluctuation in the signal. But by the time this fluctuation becomes comparable (in magnitude) to some other random fluctuations in the signal (for example, random fluctuations of the intensity of peak B) PCA does not distinguish the fluctuations produced by A as being more important or even relevant to describe the data. If there are larger peaks that are nearby or partially overlapping with the signal we want to recover (like peak B in our example here), then "small" random fluctuation (of, say, $\sim$ 10%) of the larger signal can be already larger than the fluctuations we are inducing by the electrochemical modulation of A. This explicitly shown in Fig. S4, where peak A is much weaker than peak B. Peak A can barely be seen in the average spectrum (Fig. S4(a)), and it is almost impossible to distinguish in individual spectra of the time series (a few examples of which are shown in Fig. S4(b)). A straight PCA analysis of this situation results in the eigenvectors displayed Fig. S4(c) (where we show the first four PCA eigenvectors in order of importance). While there is a hint of the presence of peak A in the first one (which represents the average spectrum[19]), the following eigenvectors are concerned with trying to model the random fluctuations of peak B arround the average (which are deemed to be more important as far as contributions to the variance of the signal is concerned). It is always possible that a hint of peak A will exist at some point for higher order eigenvectors; but even in this situation the contributions from peak A appear mixed among several eigenvectors with additional structures related to random fluctuations of peak B of the same order of importance. Accordingly, PCA reaches here a limit to analyze and separate the different independent contributions to the spectra.

This is the point where we can combine PCA with a previous pre-filtering from FFT, and this is explicitly shown in Fig. S5. From the integrated intensity of the spectra as a function of time shown in Fig. S5(a) (which in this case is contributed mainly by peak B and its modulation due a partial charge transfer) we can deduce the *electrochemical modulation frequency* of the spectra by a standard FFT transformation. This is explicitly shown in Fig. S5(b), where two clear (symmetric with respect to the middle) satellite peaks representing the main FFT frequency of the modulation can be clearly identified. We can then followed the standard procedure of frequency filtering: (*i*) We do a pixel-by-pixel FFT and in all of them we multiply the signal by a frequency filter that eliminates all FFT-frequencies except the two shown in in Fig. S5(b). (*ii*) We transform back each pixel of the spectra back to the time domain; thus achieving a temporal sequence of spectra that is "locked-in" with the electrochemical modulation frequency. (*iii*) We finally PCA the FFT-filtered data

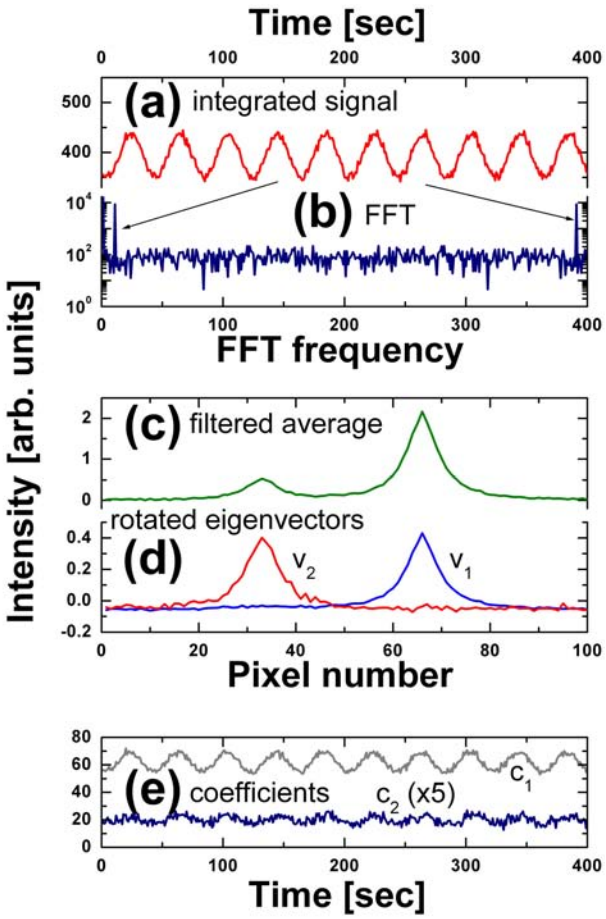

FIG. S5: (a) The time variation of the total integrated intensity of each spectrum (which is mainly contributed by peak B) can be used to determine the main FFT frequency of the modulation; shown as two spikes in the FFT spectrum in (b). The original signal can be filtered at this frequency in *each* pixel, and transformed back to the time domain by an inverse FFT transform. The resulting average spectrum in (c) of the FFT-filtered signal contains a much larger contribution of peak A with respect to peak B. This is because only the "modulated" part of the total intensity of peak B survives the filtering. As a result, the contribution to fluctuations of peak A is (in relative terms) "enhanced" after filtering. A PCA analysis of the filtered data now identifies clearly the two contributions; the rotated eigenvectors [19] in (d) can be used now to represent the signal through the coefficients displayed in (e) (note that c_2 has been multiplied by five). Most of the signal is still contributed by B and its partial charge transfer modulation, but the contribution from A can be clearly lifted from the background fluctuations. See the text for further details.

in search for the principal eigenvectors that describe the data.

It is instructive to look at the temporal average of the spectra after they had been FFT-filtered, and this is shown in Fig. S5(c). If we compare this average with Fig. S4(a), we notice that the relative intensity of peak

A has increased with respect to B. This is because only the fraction of the intensity of peak B that is at the right modulation frequency survives. All other random modulations of the intensity –that were contributing to the variance in the unfiltered PCA– are now removed. As explained in the main text, we are "preselecting" the type of fluctuations that we are going to analyze with PCA in a second step. This filtering enhances the importance of the fluctuations of peak A to the variance (because they are now at the right frequency) and can be, hence, picked up by PCA as one of the principal contributions. PCA is basically blind to the time sequence of the electrochemical modulation. If we were to scramble all the spectra in the time sequence and do PCA on the result, we would have exactly the same result. The calculation of the covariance matrix in PCA [19] is insensitive to the time ordering of the spectra. But adding a pre-filtering of the fluctuations with FFT is helping PCA to assign an importance to the correlations in the variations of intensity that are at the right electrochemical modulation frequency. In this manner, very small signals can be "amplified" and identified. This is nothing but (in a very rudimentary implementation) the basic operation of the lock-in amplifier applied on a pixel-by-pixel basis (before PCA). The main differences with respect to a lock-in amplification are that: (*i*) it is not done in real time, and (*ii*) it is done here with a much smaller sampling of only a few periods (as compared to lock-in modulations that can reach KHz and MHz in some cases). A shorter (summarized) version of this reasoning is given in the main text of the paper.

Form here onwards, the analysis proceeds as in standard PCA. Fig. S5(d) shows the two main eigenvectors detected by PCA in the FFT-filtered data (after a suitable rotation [19]), and Fig. S5(e) shows the coefficients of the decomposition of the intensity of the spectra as a function of time in terms of these two eigenvectors. The two contributions can be clearly separated, and the phase-lag of the electrochemical modulation of both species revealed. Hence, even when peak A has a negligible contribution to the overall intensity of the spectra, it can be identified as isolated: a task that is only possible due to the ability to modulate its intensity (electrochemically) at a well specified frequency. This latter example is basically similar to the experimental case of the combination of NB (at low concentrations) and CV treated in the main text.

[1] F. Ni, H. Feng, L. Gorton, and T. M. Cotton, Langmuir **6**, 66 (1990).

[2] L. Gorton, A. Torstensson, H. Jaegfeldt, and G. Johansson, J. Electroanal. Chem. **161**, 103 (1984).

[3] H. H. Liu, J. L. Lu, M. Zhang, and D. W. Pang, Analytical Sciences **18**, 1339 (2002).

[4] L. Gorton, J. Chem. Soc., Faraday Trans. **82**, 1245 (1986).

[5] T. Sagma, S. Igarashi, H. Sato, and K. Niki, Langmuir **7**, 1005 (1991).

[6] L. Li, X. Tian, G. Zou, Z. Shi, X. Zhang, and W. Jin, Anal. Chem. **80**, 3999 (2008).

[7] J. S. Yu and T. Y. Zhou, J. of Electroanal. Chem. **504**, 89 (2001).

[8] D. P. dos Santos, G. F. S. Andrade, M. L. A. Temperini, and A. G. Brolo, J. Phys. Chem. C **113**, 17737 (2009).

[9] P. D. Lacharmoise, P. G. Etchegoin, and E. C. Le Ru, ACS Nano **3**, 66 (2009).

[10] T. Watanabe and B. Pettinger, Chem. Phys. Lett. **89**, 501 (1982).

[11] M. V. Cañamares, C. Chenal, R. L. Birke, and J. R. Lombardi, J. Phys. Chem. C **112**, 20295 (2008).

[12] W. Sun, Y. Ding, and K. Jiao, J. of Anal. Chem. **61**, 359 (2006).

[13] H. Watanabe, N. Hayazawa, Y. Inouye, and S. Kawata, J. Phys. Chem. B **109**, 5012 (2005).

[14] I. T. Jolliffe, *Principal Component Analysis* (Springer Verlag, Berlin, 2002).

[15] A. Hyvärinen, J. Karhunen, and E. Oja, *Independent Component Analysis* (John Wiley & Sons, New York, 2001).

[16] W. H. Press, B. P. Flannery, S. A. Teukolsky, and W. T. Vetterling, *Numerical Recipes in FORTRAN: The Art of Scientific Computing* (Cambridge University Press, Cambridge, 1989).

[17] E. Kreyszig, *Advanced Engineering Mathematics, 9$^{\text{th}}$-edition* (John Wiley & Sons, New York, 2006).

[18] J. Kauppinen and J. Partanen, *Fourier Transforms in Spectroscopy* (Wiley-VCH Verlag, Berlin, 2001).

[19] P. G. Etchegoin, M. Meyer, E. Blackie, and E. C. Le Ru, Anal. Chem. **79**, 8411 (2007).